ELSEVIER

NeuroImage

www.elsevier.com/locate/ynimg
NeuroImage 21 (2004) 144–153

Discrepancies between BOLD and flow dynamics in primary and supplementary motor areas: application of the balloon model to the interpretation of BOLD transients

Takayuki Obata,* Thomas T. Liu, Karla L. Miller, Wen-Ming Luh, Eric C. Wong, Lawrence R. Frank, and Richard B. Buxton

Department of Radiology, University of California at San Diego, La Jolla, CA 92039-0677, USA

Received 8 April 2003; revised 18 August 2003; accepted 28 August 2003

The blood-oxygen-level-dependent (BOLD) signal measured in the brain with functional magnetic resonance imaging (fMRI) during an activation experiment often exhibits pronounced transients at the beginning and end of the stimulus. Such transients could be a reflection of transients in the underlying neural activity, or they could result from transients in cerebral blood flow (CBF), cerebral metabolic rate of oxygen ($CMRO_2$), or cerebral blood volume (CBV). These transients were investigated using an arterial spin labeling (ASL) method that allows simultaneous measurements of BOLD and CBF responses. Responses to a finger-tapping task (40-s stimulus, 80-s rest) were measured in primary motor area (M1) and supplementary motor area (SMA) in five healthy volunteers. In SMA, the average BOLD response was pronounced near the beginning and end of the stimulus, while in M1, the BOLD response was nearly flat. However, CBF responses in the two regions were rather similar, and did not exhibit the same transient features as the BOLD response in SMA. Because this suggests a hemodynamic rather than a neural origin for the transients of the BOLD response in SMA, we used a generalization of the balloon model to test the degree of hemodynamic transients required to produce the measured curves. Both data sets could be approximated with modest differences in the shapes of the $CMRO_2$ and CBV responses. This study illustrates the utility and the limitations of using theoretical models combined with ASL techniques to understand the dynamics of the BOLD response.

Keywords: Flow dynamics; Balloon model; BOLD transients

Introduction

The blood-oxygenation-level-dependent (BOLD) effect on the signal measured with magnetic resonance imaging (MRI) is widely used for mapping patterns of activation in the human brain. The source of the BOLD effect is thought to be primarily due to changes in local deoxyhemoglobin content, which alters the magnetic susceptibility of the blood and creates local magnetic field gradients around the vessels that alter the MR signal. However, quantitative links between the underlying neural activity and the resulting physiological changes in cerebral blood flow (CBF), cerebral metabolic rate of oxygen ($CMRO_2$), and cerebral blood volume (CBV) are still poorly understood. In particular, the BOLD response to brain activation often exhibits transient features, such as overshoots and undershoots, which differ from the shape of the stimulus (e.g., a square wave) (Frahm et al., 1996; Kruger et al., 1996). Such features could result if the neural response itself is related to the stimulus in a nonlinear way, so that these transient features are intrinsic to the neural activity (Boynton et al., 1996; Miller et al., 2001). However, because the change in local deoxyhemoglobin content depends on the combined changes in CBF, $CMRO_2$, and CBV, transients in the BOLD response could arise from transients in any of these three physiological variables as well. For example, in animal studies with an intravascular marker, Mandeville et al. (1998) found that the dynamics of the CBV change does not match the dynamics of the CBF change. This experimental finding was the basis for two similar theoretical models, the balloon model (Buxton et al., 1998b) and the delayed compliance model (Mandeville et al., 1999), which attempt to explain the post-stimulus undershoot of the BOLD response in terms of a CBV response that recovers to baseline more slowly than the CBF response.

Recently, Nakai et al. (2000) reported unique BOLD signal changes in the supplementary motor cortex area (SMA), where they observed overshoots at both the beginning and end of a finger-tapping stimulus. This pattern could be due to more intense neural activity at the beginning and end of the motor activity (the transition points). However, given the complexity of the relationship between the BOLD response and the underlying changes in hemodynamics and oxygen metabolism, it is not possible to rule out a hemodynamic explanation. To explore this phenomenon in more detail, we have combined MRI techniques for measuring CBF with BOLD measurements to try to unravel the source of these transients. Using these arterial spin labeling (ASL) methods,

* Corresponding author. Department of Medical Imaging, National Institute of Radiological Sciences, 4-9-1 Anagawa, Inage, Chiba 263-8555, Japan. Fax: +81-43-251-7147.
E-mail address: t_obata@nirs.go.jp (T. Obata).
Available online on ScienceDirect (www.sciencedirect.com.)

1053-8119/$ - see front matter © 2003 Elsevier Inc. All rights reserved.
doi:10.1016/j.neuroimage.2003.08.040

it is possible to measure both CBF and BOLD time course from the same data set. In a preliminary study (Obata et al., 2000), we re-examined our previously reported data to look specifically at the activity in SMA. From this limited data, there was evidence for overshoots of the CBF signal at the beginning and end of the stimulus, which would support the view that these transients are neural in origin (i.e., that neural overshoots drive a CBF overshoot which then drives a BOLD response overshoot). However, to more fully test this idea, we conducted a prospective study in healthy volunteers using a different ASL approach for measuring the CBF and BOLD responses that eliminate potential cross-contamination between the two measurements. In this more systematic study, we found no evidence for overshoot transients in the CBF signal. If the CBF does not show these transients, the more likely explanation for the BOLD transients is that they are due to transient features of the CBV or $CMRO_2$ response. To test this idea, we modeled our experimental results with a generalized and updated version of the balloon model.

Materials and methods

Pulse sequence for measuring BOLD and flow signals

In arterial-spin-labeling (ASL) pulse sequences, arterial blood is tagged proximal to the imaging slice by inversion of the magnetization, and sequential images are acquired in which blood magnetization is alternately inverted and not inverted (see Buxton, 2002 for a review). We refer to these as tag and control states, respectively. Subtraction of tag from control images then leaves a difference signal ΔM that is proportional to local CBF (Buxton et al., 1998a; Wong et al., 1997). For an activation experiment, images are acquired dynamically during the task, alternating between tag and control images. From this time series, the CBF time series is constructed by taking the difference of the tag and control signals, and a BOLD time series is constructed by taking the average of the tag and control signals.

For these experiments, we used a dual-echo, single-shot, spiral *k*-space trajectory pulse sequence, an approach originally proposed by Glover et al. (1996). When implemented in an ASL experiment, the first echo encodes the CBF signal alone, while the second echo with longer TE is also sensitive to the BOLD effect. This differs from our previous approach to measuring both CBF and BOLD responses in which we used a single acquisition at TE = 30 ms (Buxton et al., 1998b). The dual-echo spiral approach provides a CBF signal that is minimally contaminated by BOLD effects because of the short TE.

A potential problem with quantifying CBF with ASL methods is the effect of variable transit delays for blood to travel from the tagging region to the imaged section. We controlled for this using the PICORE-QUIPSS II technique (Wong et al., 1997, 1998a,b), illustrated in Fig. 1. This pulse sequence begins with a 90° saturation pulse on the section to be imaged to reduce the signal of static spins. A 180° inversion pulse is then applied to a tagging band below the section to be imaged. After waiting a time TI_1 to allow tagged arterial blood to move out of the tagging band, a 90° saturation pulse is applied to the tagging band (in our implementation, two 90° pulses are applied in quick succession to improve the saturation). This destroys the longitudinal magnetization of any tagged arterial blood still in the tagging band, and so creates a well-defined bolus of tagged blood with duration TI_1. At time TI_2 after the initial inversion pulse, the images are collected with a dual-echo spiral *k*-space trajectory. Provided that the interval $TI_2 - TI_1$ is longer than the transit delay from the tagging band to the imaged slice, all of the bolus will be delivered and the total volume delivered is directly proportional to CBF, with minimal sensitivity to the transit delay (Wong et al., 1997, 1998a,b). For control images, the acquisition is the same except that the 180° inversion pulse is applied off-resonance and with no gradient pulses applied (Wong et al., 1997). In this way, off-resonance effects on the static spins are the same, but no spins are tagged. The data acquisition alternates between tag and control images throughout the experimental run.

Data collection and analysis

The data were obtained on a 1.5 T imager using a spiral QUIPSS II (TE1 = 2 ms, TE2 = 30 ms, TR = 2 s, FOV = 24 cm, matrix = 64 × 64, TI1 = 700 ms, TI2 = 1400 ms) pulse sequence.

The BOLD and flow data were collected on five subjects performing a bilateral sequential finger-tapping task. Informed consent was obtained from all subjects before the experiment according to the guidelines of our institutional review board. The task for each subject consisted of four sets of four cycles of 40 s of finger tapping followed by 80 s of rest (a total of 16 activation blocks). The long rest period between activation blocks is necessary to fully resolve the post-stimulus undershoot of the BOLD signal. For each subject, all of the data were re-aligned in post-processing using standard routines in the AFNI analysis package (Cox, 1996). Data for each subject were then averaged across experimental runs. For the average 8-min run, a flow time series (control − tag) and a BOLD time series (control + tag) were then calculated for each image voxel. For the flow time series, the first echo signal at each measured time point was subtracted from the average of the signals just before and just after that time point, with the sign adjusted to make each subtraction equivalent to control minus tag. For the BOLD time series, the second echo signal at each time point was averaged with the average of the signals just before and after that time point.

Activated pixels in SMA and M1 were identified from the flow changes by a Student *t* test analysis between baseline and activating points (threshold: $t > 5.2$, $P < 5 \times 10^{-6}$). To avoid any influence from potential overshoots, only 10 central time points during the stimulation (16–34 s after stimulation onset) and 25 baseline points well-removed from the post-stimulus undershoot (72–120 s after stimulation onset) were used in the analysis. The BOLD signal change was normalized as percent change from baseline in each pixel and flow is normalized to the average resting flow signal in the brain in each subject. The time courses for all activated pixels were averaged across all subjects to create a single time course.

Model analysis

The BOLD signal changes were analyzed using a model that describes the effects of hemodynamic changes on the BOLD signal, the balloon model (Buxton et al., 1998b). It is assumed in the model that the vascular bed (CBV) within a small volume of tissue can be modeled as an expandable venous compartment (a balloon) that is fed by the output of the capillary bed. The model is defined in terms of the total volume of the balloon (v) and the total deoxyhemoglobin within the balloon (q). The dynamic changes in v and q are driven

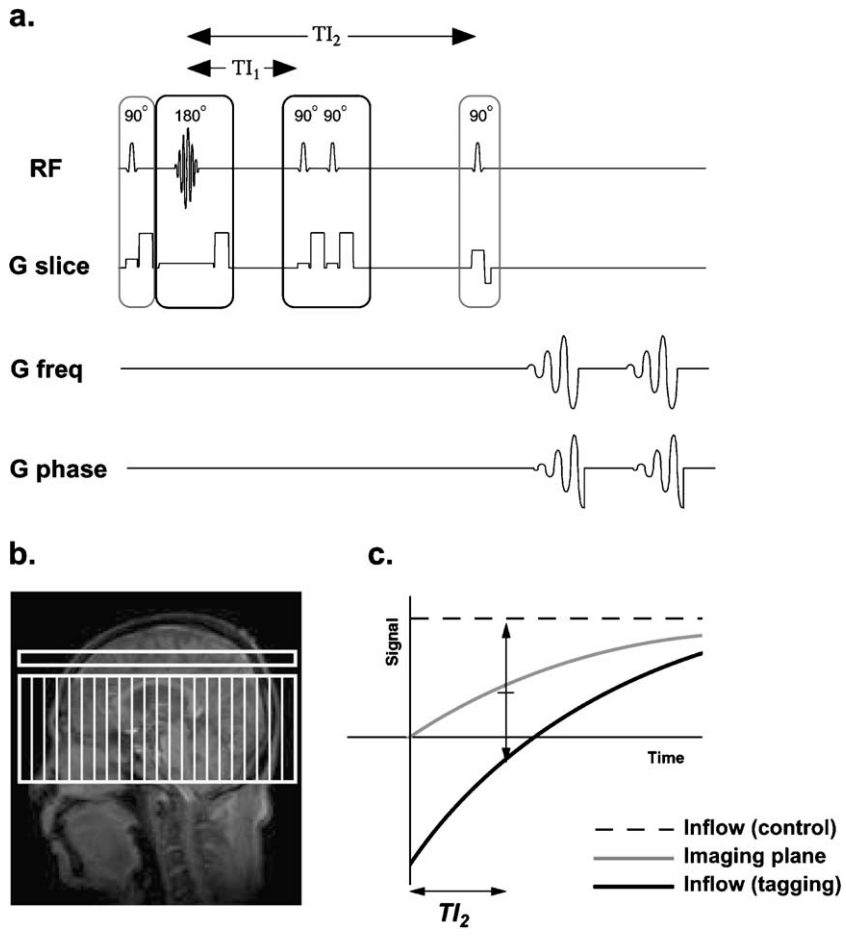

Fig. 1. Pulse sequence for QUIPSS II. RF pulses (from left to right) are (1) in-plane pre-saturation sinc pulse on the image plane (open box in b); (2) inversion tag or control hyperbolic secant pulse on the tagging band (striped box in b); (3–4) double saturation (two sequential 90° sinc pulses) in the tagging band; (5) 90° excitation sinc pulse in the image plane. Data are collected with a dual-echo spiral readout. (c) Illustrates the magnetization recovery of arterial blood in the tag part of the experiment (black), arterial blood in the control part of the experiment (dashed), and static spins in the image plane (gray). The signals are measured at time TI_2 (arrow in c). Subtraction of tag and control signals removes the static spin signal (which is the same in both experiments) and leaves a signal proportional to CBF. Averaging the tag and control signals produces an average recovery curve that approximates the saturation recovery curve of the static spins, and so produces a BOLD curve with minimal flow weighting.

by changes in CBF, CBV, and $CMRO_2$ associated with brain activation. The equations of the balloon model represent mass conservation for blood and deoxyhemoglobin as they pass through the venous balloon:

$$\frac{dq}{dt} = \frac{1}{\tau_0}\left[f_{in}(t)\frac{E(t)}{E_0} - \frac{q(t)}{v(t)}f_{out}(v,t)\right]$$

$$\frac{dv}{dt} = \frac{1}{\tau_0}\left[f_{in}(t) - f_{out}(v,t)\right] \quad (1)$$

In these equations, q is the total deoxyhemoglobin within the balloon, v is the volume of the balloon, f_{in} is the inflow, and f_{out} is the outflow from the balloon. Each of these quantities is normalized to its value at rest, so each is dimensionless and before activation $q = v = f_{in} = f_{out} = 1$. The net extraction fraction of oxygen is $E(t)$, and the resting value is typically $E_0 = 0.4$. The time dimension of the equations is scaled by the time constant τ_0, the mean transit time through the balloon at rest. For a cerebral blood flow of 60 ml/min–100 ml of tissue (equivalent to a rate constant of 0.01 s^{-1}) and a resting venous blood volume fraction of $V_0 = 0.02$, the mean transit time is $\tau_0 = 2$ s.

The driving function of the system is the quantity $f_{in}(t)E(t)$. In the original formulation of the balloon model (Buxton et al., 1998b), the extraction fraction was modeled as a fixed function of the inflow f_{in}, a tight coupling of flow and oxygen metabolism. To generalize the equations, we treat $E(t)$ as an independent quantity to be able to explore the dynamics that result from uncoupling of blood flow and oxygen metabolism. Note that the quantity $f_{in}E / E_0$ is simply the cerebral metabolic rate of oxygen ($CMRO_2$) normalized to its value at rest.

We modeled the BOLD signal as a function of $q(t)$ and $v(t)$ with a modified form of the model described originally (Buxton et al., 1998b). This new form of the BOLD signal model corrects an error in the previous formulation, makes less approximations in the linearization of the signal, and uses newer data from the literature in the estimates of the model parameters. Because this new formulation differs in several respects from the original, including the final form of the model, we include a full derivation in the

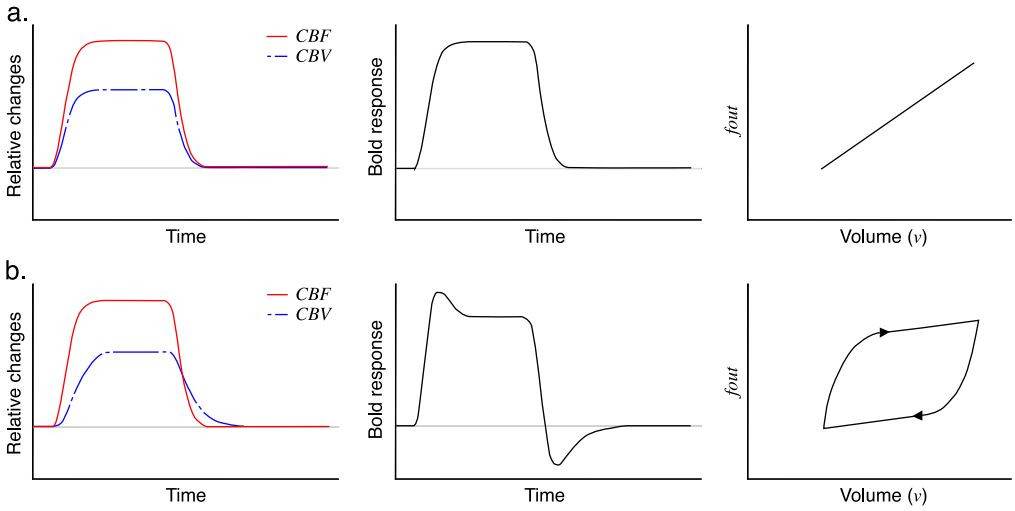

Fig. 2. Balloon model curves illustrating BOLD response transients in the absence of flow transients. The left column shows time courses for the volume of the local venous component (CBV, or $v(t)$ in Eq. (1)) and blood flow into the tissue (CBF, or $f_{in}(t)$ in Eq. (1)), the center column shows the resulting blood-oxygen-level-dependent (BOLD) signal response, and the right column shows the relationship between outflow ($f_{out}(v)$ in Eq. (1)) and blood volume (v). (a) A model in which CBV closely follows CBF. (b) A model in which CBV changes lag behind CBF changes, producing strong transients in the BOLD response. For this model, the function $f_{out}(v)$ shows hysteresis analogous to a viscoelastic effect that resists sudden changes in volume (right column). In both of these models, the oxygen extraction fraction $E(t)$ is coupled to $f_{in}(t)$ such that the fractional CBF change is always three times larger than the fractional $CMRO_2$ change.

Appendix A. Based on this model, the BOLD signal change as a fraction of the resting signal can be approximated as:

$$\frac{\Delta S}{S} \approx V_0[a_1(1-q) - a_2(1-v)] \quad (2)$$

where V_0 is the resting volume fraction of the balloon, and the dimensionless parameters a_1 and a_2 depend on several experimental and physiological parameters. The values estimated in the Appendix for a magnetic field of 1.5 T with TE = 40 ms and $E_0 = 0.4$ are $a_1 = 3.4$ and $a_2 = 1.0$. In Eq. (2), the first term describes the primary dependence on the total amount of deoxy-hemoglobin, while the second term is a smaller correction for the effect of a blood volume change.

Eqs. (1) and (2) provide a flexible mathematical framework for exploring how the BOLD signal change ($\Delta S/S$) results from dynamic changes in CBF ($f_{in}(t)$), CBV ($v(t)$), and $CMRO_2$ (modeled by a dynamic oxygen extraction fraction $E(t)$). Fig. 2 shows a simple example of how a CBV change that lags behind the CBF change can produce both an initial overshoot and a post-stimulus undershoot of the BOLD signal, even when the CBF response shows neither of these effects.

Results

Experimental results

Across the five subjects, 34 pixels in SMA and 98 pixels in M1 passed the criteria for activation, and the average curves for flow and BOLD are shown in Fig. 3. The qualitative result is that the flow curves for M1 and SMA are rather similar, but the BOLD curves are distinctly different, with the SMA BOLD signal exhibiting a strong initial overshoot, a gradual increasing ramp during the stimulus, and a smaller post-stimulus undershoot than was observed in M1. There was no evidence for the initial overshoot in the flow data from SMA. To test the significance of these observed changes in the response profile, mean values were calculated for four intervals after the onset of stimulation, defined as early (6–12 s), middle (18–30 s), late (40–46 s), and undershoot (58–64 s). These intervals correspond to the transient features seen in SMA, and the mean and standard errors are listed in Table 1. For the SMA BOLD curve, the early and late portions of the curve were significantly stronger than the middle portion (t = 3.3, 3.2, respectively, $n = 5$, $P < 0.05$, paired t test), and the post-stimulus undershoot was significantly smaller than the undershoot seen in M1 ($t = 2.8$, $P < 0.05$, paired t test).

The flow responses in SMA and M1 were rather similar, except that the M1 response returned to baseline more quickly and showed evidence of a small, brief post-stimulus undershoot (although this did not reach statistical significance). In short, the key finding was that the flow responses in the two regions were rather similar, but the BOLD responses were quite different.

Modeling results

We used the balloon model to try to understand how similar flow responses could lead to such different BOLD responses. Fig. 4 shows three models in which the time courses for the CBF, CBV, and $CMRO_2$ responses are slightly different. In Fig. 4a, $f_{in}(t)$ was chosen to match the experimental CBF curve measured in M1, including a weak post-stimulus undershoot. In this model, the $CMRO_2$ response closely follows the CBF response, but with a reduced magnitude. The CBV response is slightly delayed from the CBF response, returning to baseline more slowly. The resulting theoretical BOLD response approximates the measured BOLD response in M1, including an amplified post-stimulus undershoot.

Figs. 4b and c show two models for the SMA response, with $f_{in}(t)$ chosen to match the experimentally determined CBF re-

sponse. In each model, the CBV response lags behind the CBF response, creating the initial BOLD overshoot and the BOLD post-stimulus undershoot. The BOLD overshoot at the end of the stimulus occurs in these models because either the $CMRO_2$ or the CBV fails to follow the CBF as it slowly increases during the stimulus. Fig. 4b shows a model in which $CMRO_2$ reaches a plateau, and Fig. 4c shows a model in which CBV reaches a plateau. With either model, the resulting BOLD responses are nearly identical. Note that these are just two examples of CBV and $CMRO_2$ responses that could produce a BOLD response similar to what we measured in SMA. Increasing $CMRO_2$ and increasing CBV both increase the total deoxyhemoglobin, so increasing either one will have similar (although not identical) effects on the BOLD signal. What appears to be required to model the SMA BOLD response is that the total deoxyhemoglobin does not increase as fast as the CBF during the stimulus. We have modeled this by requiring either $CMRO_2$ or CBV to reach a plateau, but a similar BOLD response would occur if both quantities continued to increase, but at a slower rate.

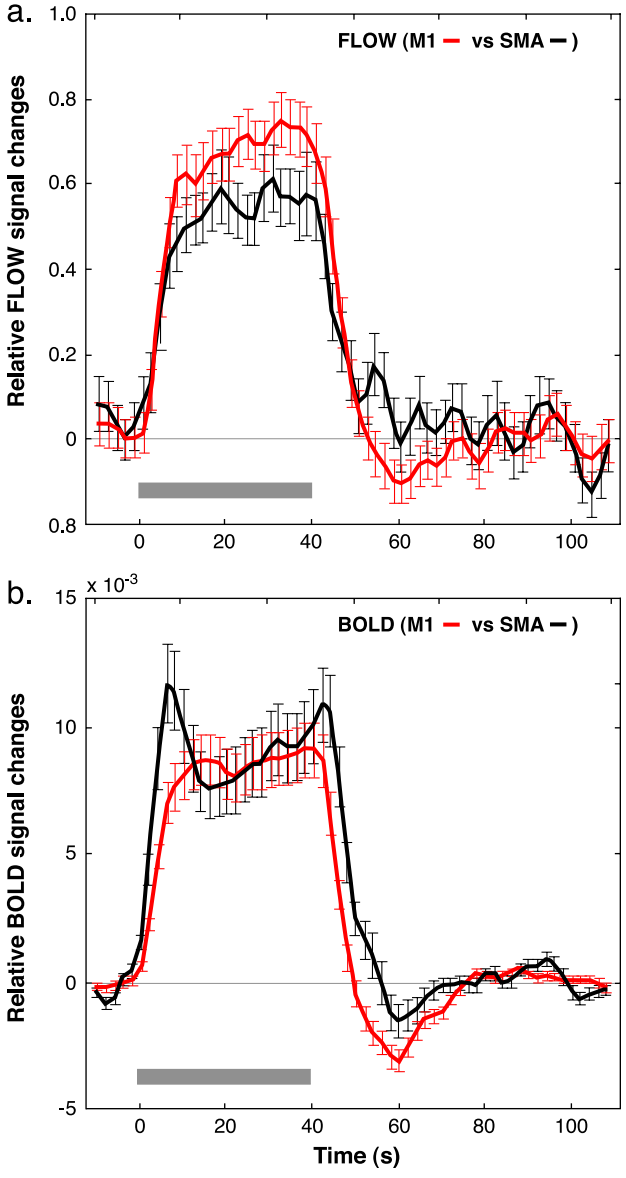

Fig. 3. Average BOLD and CBF time courses and standard errors measured in primary motor area (M1) and supplementary motor areas (SMA). (a) Flow time course and (b) BOLD time course for both areas. The BOLD response in SMA shows a different pattern of transients than that seen in M1 (b), but the flow responses in the two regions are rather similar (a). In particular, the prominent transients of the BOLD response in SMA are not present in the flow response.

Table 1
Percent changes relative to baseline

	Early (6–12 s)	Middle (18–30 s)	Late (40–46 s)	Undershoot (58–64 s)
Flow SMA	47.00 (5.71)	57.39 (8.89)	45.43 (11.32)	1.79 (3.70)
Flow M1	61.73 (8.38)	71.31 (8.22)	60.25 (9.36)	− 10.71 (4.18)
BOLD SMA	1.07 (0.15)*	0.78 (0.11)	1.03 (0.13)*	− 0.11 (0.12)**
BOLD M1	0.83 (0.15)	0.91 (0.15)	0.89 (0.16)	− 0.28 (0.10)**

Percent changes (standard error) in each period relative to baseline (72–120 s after onset of stimulation).
* Significantly larger ($P < 0.05$) than the value in the middle period.
** Significantly different ($P < 0.05$) between SMA and M1.

Discussion

The BOLD response to brain activation often contains transient features, the most prominent being a post-stimulus undershoot. The cause of these transients is still debated, but a likely source is that the physiological changes in CBF, $CMRO_2$, and CBV that combine to form the BOLD response may have different time courses. However, such BOLD transients could reflect transient features of the underlying neural activity. From measurements of the BOLD signal alone, it is not possible to distinguish among these different possible sources. To explore these issues in a quantitative way, we have taken as a test case the comparison of BOLD responses in primary and supplementary motor areas, prompted by reports of significantly different BOLD responses to the same stimuli (Nakai et al., 2000). Specifically, the BOLD response in SMA showed overshoots at the beginning and end of a motor stimulus that were not present in the BOLD signal from M1.

We used an arterial spin labeling technique to simultaneously measure the BOLD and CBF signal changes in SMA and M1 during a simple bilateral finger-tapping stimulation. The CBF responses in SMA and M1 were similar, although the M1 response exhibited a slight post-stimulus undershoot. However, the BOLD responses in the three regions were distinctly different. In SMA, the BOLD signal exhibited an overshoot at the beginning of the stimulus, a gradual increasing ramp during the stimulus, and a small undershoot after the end of the stimulus. In contrast, the BOLD signal in M1 did not show the initial overshoot, and showed a more pronounced post-stimulus undershoot.

The significant differences between the CBF and BOLD responses in SMA are also unlikely to be due to systematic error. By using a dual echo image acquisition and deriving the CBF time course from the first echo, there is little contamination by the BOLD effect. In any functional magnetic resonance imaging (fMRI)

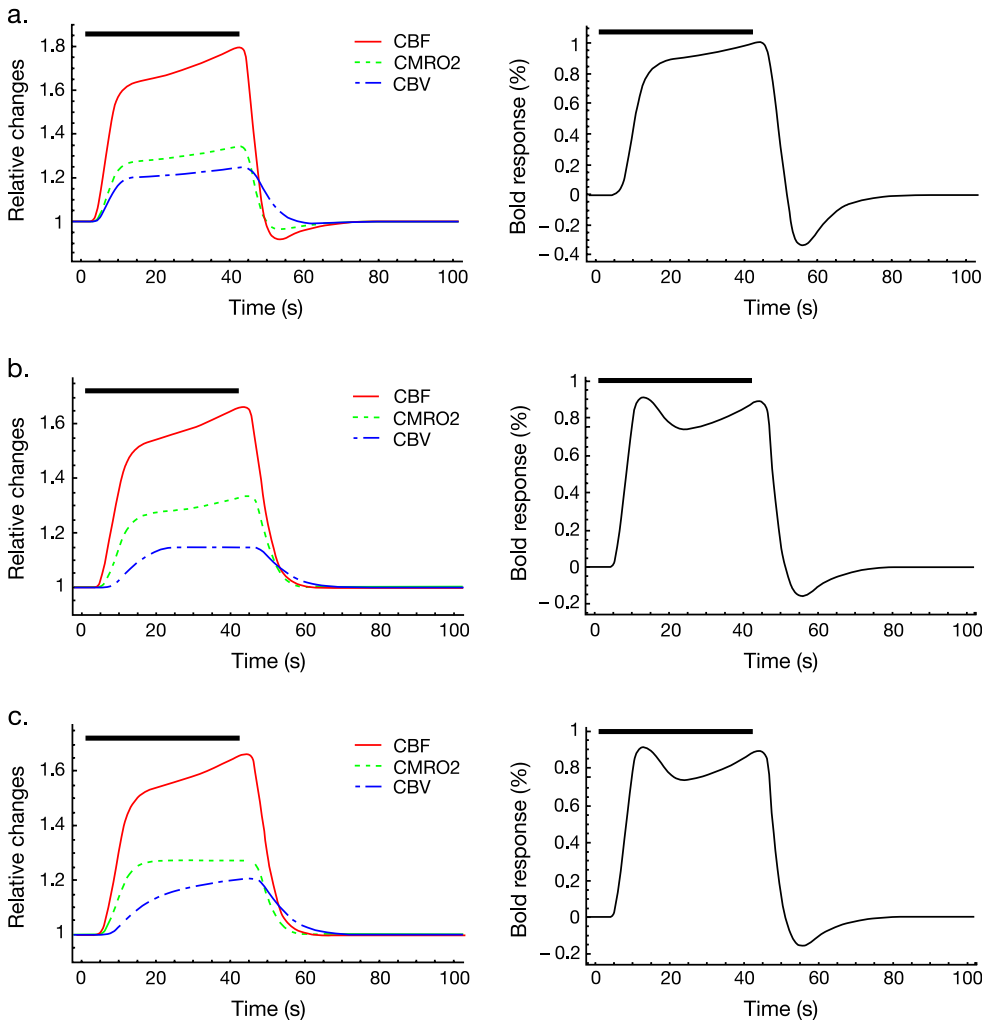

Fig. 4. Balloon model curves modeling the M1 and SMA data. Time courses of cerebral blood flow, volume, and metabolic rate of oxygen (CBF, CBV, and $CMRO_2$; left column), and corresponding blood-oxygen-level-dependent (BOLD; right column) signal change calculated with the balloon model. Each CBF curve has the same shape as the corresponding measured signal time course. (a) A model for M1, in which CBF and $CMRO_2$ are closely coupled, but CBV changes lag behind CBF changes. (b) A model for SMA, in which $CMRO_2$ and CBF are coupled, but the CBV change plateaus as CBF continues to increase. (c) A model in which CMRO2 plateaus while CBF continues to increase. Note that the rather different physiological models in b and c produce nearly identical BOLD responses.

experiment in which active voxels are identified by correlation analysis and an average response is calculated, there is a risk of introducing a bias into the calculated average response. If one locates all voxels that correlate with a particular response shape, then there is a bias for the average of those selected curves to resemble the chosen shape. To avoid this type of bias, we used only time points in the middle of the stimulus and long after the end of the stimulus to avoid the transient effects under investigation. In addition, we only used the flow response for voxel selection, so the derived BOLD curves should be completely unbiased. Finally, all of these responses were measured simultaneously for the same stimuli, so there should be no errors introduced from comparing results from different experiments.

A critical feature of all ASL studies is the need to control for differences in transit delay from the tagging region to the image plane. With the QUIPSS II protocol used, differences in transit delay should have little effect on the measured CBF changes provided that these transit delays are shorter than TI2 − TI1, which was 700 ms in these studies. In principle, if the transit delay to SMA is longer, the flow measurements could be in error. Specifically, if the transit delay is longer than 700 ms at rest and is then reduced with activation, the fractional change in flow would be overestimated because not all of the tagged spins were being measured at rest. However, this potential overestimate of flow cannot account for the missing initial flow overshoot in SMA, which would require an underestimate of flow.

These results indicate that hemodynamic responses in SMA and M1 for the same stimulus are different. One possible explanation for this difference is that neural activity in SMA is higher at the beginning and end of the stimulus, when SMA is exerting control over M1, while the neural activity in M1 is more continuous. If so, then we would predict that the CBF response should reflect this neural activity response, and indeed, this was our hypothesis as we began this study. However, the data do not support this conclusion. Instead, CBF responses are rather similar in the two regions (although not identical), and there is no

evidence for a flow overshoot at the beginning or end of the stimulus.

These unexpected results led us to investigate theoretically how different the time course of CBF, $CMRO_2$, and CBV would have to be to produce such different BOLD responses for similar flow responses. To do this, we used a generalized version of the balloon model to compute curves of blood volume ($v(t)$) and total deoxyhemoglobin ($q(t)$) for different assumed curves for CBF, $CMRO_2$, and CBV. The dynamic curves for $v(t)$ and $q(t)$ were then used to calculate the BOLD response using a new model for the BOLD signal that corrected some deficiencies of the original signal model presented earlier (Buxton et al., 1998b). The approach developed here is a general mathematical framework that can be applied to other studies modeling the BOLD effect.

Based on balloon model calculations, the BOLD time course in M1 is consistent with a $CMRO_2$ curve that closely follows the CBF curve but with one-third of the magnitude, and a CBV curve that lags behind the CBF curve. These physiological curves are similar to ratios of CBF to $CMRO_2$ change measured with a calibrated BOLD experiment (Davis et al., 1998) and to delayed CBV recovery curves measured in animal studies with intravascular contrast agents (Mandeville et al., 1998). Note also that the magnitude of the post-stimulus undershoot, as a fraction of the peak response, is substantially larger in the BOLD response than in the CBF response in both the data and the model curves. This is because there are two sources of the BOLD post-stimulus undershoot: the undershoot of CBF and the slow return of CBV to baseline.

Modeling the BOLD response in SMA required a more significant uncoupling of CBF and either $CMRO_2$ or CBV. Specifically, to match the continual rise of the BOLD response during the stimulus required that the rise of either $CMRO_2$ or CBV was capped. Note, though, that other families of curves are possible in which both $CMRO_2$ and CBV continue to rise, but at a slower rate. It is worth pointing out that the model in which CBV reaches a maximum, and does not continue to increase as CBF increases, may also provide part of the explanation for why the post-stimulus undershoot in M1 is not seen in SMA. Part of the explanation for the undershoot in M1 is the undershoot of the CBF signal there, but the second part is due to the increased CBV, which increases local deoxyhemoglobin content. If the CBV does not increase as much, this effect is reduced. Another factor that could affect the post-stimulus undershoot if it is due to slow CBV changes is that the CBF itself is slower to return to baseline in SMA. That is, by this model (and the delayed compliance model), the post-stimulus undershoot reflects the difference in recovery times of CBF and CBV, and for SMA, the CBF recovers more slowly, like the CBV. Finally, it is important to note that while the post-stimulus undershoot here is modeled as a slow return of CBV to baseline, such a transient could in principle be due to a slow return of $CMRO_2$ to baseline (Frahm et al., 1996).

These numerical simulations show that only modest differences in the time courses of $CMRO_2$ or CBV are required to produce the observed divergence of BOLD responses in the presence of similar CBF responses (for example, compare Figs. 3a and b). This variability of response could reflect a somewhat different coupling of CBF and $CMRO_2$ in these two brain regions, although the difference would not be large. The linkage among neural activity, CBF, and $CMRO_2$ is still poorly understood, and studies such as this examining other brain regions should be helpful in defining the range of variation in CBF and $CMRO_2$ time courses. In addition, other studies have reported that the hemodynamic response depends on the particular stimulus used, even in the same region (Bandettini et al., 1997; Hoge et al., 1999; Janz et al., 2000; Kruger et al., 1998). Some of these differences could well be due to differences in the neural activity response, and the use of ASL techniques can help to separate neural activity transients from the $CMRO_2$ and CBV transients modeled here.

In conclusion, this study demonstrates the difficulty of interpreting transients of the BOLD signal when this is the only information available. Either transients of the neural activity or transients of the hemodynamic responses (CBF, $CMRO_2$, and CBV) can produce radical changes in the shape of the BOLD response. The use of ASL techniques can aid in the interpretation of BOLD response shape, as in this experiment where the lack of corresponding transients in the CBF response argues against a neural origin. However, as the balloon model calculations show, there is substantial room for variability of the $CMRO_2$ and CBV responses that will yield very similar CBF and BOLD responses, so even ASL data are not sufficient to fully interpret BOLD signal transients. Additional measurements, such as CBV measurements using flow-nulling (Liu et al., 2000) or intravascular contrast agents (Mandeville et al., 1998), will be important for unraveling the sources of the BOLD response. Finally, the mathematical framework presented here for modeling the BOLD effect should be useful in other studies as well.

Acknowledgments

This work was supported by grant NS36722 from the NIH and a postdoctoral fellowship from the Japan Science and Technology Corporation.

Appendix A. Model for the BOLD signal

The following model is patterned after the model presented by Buxton et al. (1998b), but corrects an error in the original work, makes less approximations, and uses newer experimental data to estimate the parameters. As a result, the final form is somewhat different, and the dimensionless parameters k_1, k_2, and k_3 are defined differently.

The MR signal S_0 at rest is a weighted average of the extravascular and intravascular signals (S_E and S_I, respectively):

$$S_0 = (1 - V_0)S_E + V_0 S_I \tag{A1}$$

where V_0 is the resting venous blood volume fraction. The two sources of signal can be modeled as:

$$S_E = S_{E0} e^{-TE/T_{2E}^*}$$

$$S_I = S_{I0} e^{-TE/T_{2I}^*}$$

$$\varepsilon = S_I / S_E \tag{A2}$$

where T_{2E}^* is the resting extravascular apparent transverse relaxation time, T_{2I}^* is the resting intravascular relaxation time, S_{I0} and S_{E0} are the respective effective spin densities, and ε is the intrinsic ratio of blood to tissue signals at rest.

With activation, the two transverse relaxation rates ($1/T2^*$) are altered by additive amounts ΔR^*_{2E} and ΔR^*_{2I}, and the blood volume changes to a new value V. The signal S with activation is:

$$S = (1 - V)S_E e^{-TE\times\Delta R^*_{2E}} + VS_I e^{-TE\times\Delta R^*_{2I}} \quad (A3)$$

The fractional signal change is then:

$$\frac{\Delta S}{S_0} = \frac{1}{(1 - V_0 + \varepsilon V_0)}[(1 - V)e^{-TE\times\Delta R^*_{2E}} + \varepsilon V e^{-TE\times\Delta R^*_{2I}} - (1 - V_0) - \varepsilon V_0] \quad (A4)$$

This is an exact expression for the signal change. For small changes in the relaxation rate, the exponential in the extravascular term can be expanded in a linear approximation. For the extravascular change, this is a very good approximation, and even for larger intravascular signal changes, the error is not large. Furthermore, for small blood volumes (i.e., not voxels containing a large draining vein), the multiplicative factor in front is approximately one, and eliminating products of small quantities, the signal change is approximately:

$$\frac{\Delta S}{S_0} \approx -TE\times\Delta R^*_{2E} - \varepsilon V TE\times\Delta R^*_{2I} + (V_0 - V)(1 - \varepsilon) \quad (A5)$$

It remains to estimate ε, ΔR^*_{2E}, and ΔR^*_{2I}.

A.1. Extravascular signal change

From the numerical simulations of Ogawa et al. (1993), the component of the transverse relaxation due to susceptibility differences between the vessels and the surrounding tissue is $\Delta R^*_2 = 4.3vV$, where $v = v_0(1 - Y)$ is the frequency offset in Hz at the outer surface of the magnetized vessel, v_0 (=40.3 s^{-1} at 1.5 T) is the frequency offset for fully deoxygenated blood, and Y is the fractional oxygen saturation of hemoglobin. The change in relaxation rate due to the combined change in blood oxygenation and blood volume is then:

$$\Delta R^*_{2E} = 4.3v_0[V(1 - Y) - V_0(1 - Y_0)] \quad (A6)$$

where Y is the average saturation of the venous pool in the activated state. The total deoxy-hemoglobin (deoxy-Hb) content is $Q = V(1 - Y)$[Hb], where [Hb] is the effective total hemoglobin concentration in blood, and so the activated deoxy-Hb content normalized to the resting deoxy-Hb content is:

$$q = \frac{Q}{Q_0} = \frac{V(1 - Y)}{V_0(1 - Y_0)} \quad (A7)$$

With this relation and the resting extraction fraction $E_0 = 1 - Y_0$, the relaxation rate change becomes:

$$\Delta R^*_{2E} = 4.3v_0V_0E_0(q - 1) \quad (A8)$$

Note that in this equation, q is the total deoxy-hemoglobin content within the voxel, and so depends on the concentration of deoxy-Hb both within the venous blood and the venous blood volume.

A.2. Intravascular signal change

To calculate the intravascular signal, we need to know how sensitive the exponential in R^*_{2I} is to the oxygen saturation in the range $Y = 0.6–0.8$, which approximately covers the range from rest to strong activation. Recently, this dependence was measured by Li et al. (1998) in vivo in a pig model and in vitro in blood samples. From their animal data, we can make a linear approximation to the relaxation rate over this range, $R^*_{2I} = r_0[(1 - Y) - (1 - Y_0)]$, with $r_0 = 25\ s^{-1}$, or

$$\Delta R^*_{2I} \approx r_0(1 - Y_0)\left[\frac{1 - Y}{1 - Y_0} - 1\right] \quad (A9)$$

And in terms of the normalized volume $v = V/V_0$,

$$\frac{q}{v} = \frac{Q/V}{Q_0/V_0} = \frac{1 - Y}{1 - Y_0} \quad (A10)$$

So the final expression is:

$$\Delta R^*_{2I} = r_0E_0\left(\frac{q}{v} - 1\right) \quad (A11)$$

A.3. Net signal change

Combining these expressions for the intra- and extravascular relaxation changes, and using the normalized blood volume $v = V/V_0$, the net BOLD signal change is:

$$\begin{aligned}\frac{\Delta S}{S_0} &\approx -4.3v_0V_0E_0TE(q - 1) - \varepsilon V r_0E_0TE\left(\frac{q}{v} - 1\right) + (1 - \varepsilon)(V_0 - V)\\ &= V_0\left[k_1(1 - q) - k_2v\left(\frac{q}{v} - 1\right) - k_3(1 - v)\right]\\ &= V_0[(k_1 + k_2)(1 - q) - (k_2 + k_3)(1 - v)]\end{aligned} \quad (A12)$$

with

$$\begin{aligned}\frac{\Delta S}{S} &\approx -TE4.3v_0V_0E_0(q - 1) - \varepsilon V'\ TEr_0E_0\left(\frac{q}{v} - 1\right) + (1 - \varepsilon)(V_0 - V')\\ &= V_0\left[k_1(1 - q) - k_2v\left(\frac{q}{v} - 1\right) + (1 - \varepsilon)(1 - v)\right]\\ &= V_0[(k_1 + k_2)(1 - q) - (k_2 + k_3)(1 - v)]\end{aligned} \quad (A13)$$

$$k_1 = 4.3v_0E_0TE$$

$$k_2 = \varepsilon r_0E_0TE$$

$$k_3 = \varepsilon - 1$$

At a field strength of 1.5 T with TE = 40 ms, $E_0 = 0.4$, $r_0 = 25\ s^{-1}$, $\varepsilon = 1.43$, and $v_0 = 40.3\ s^{-1}$, the dimensionless parameters are $k_1 = 2.8$, $k_2 = 0.57$, and $k_3 = 0.43$. The parameter ε, the intrinsic ratio of the intravascular to the extravascular signal at rest, was estimated from $T_{2I}^{*} = 90$ ms (Li et al., 1998) and an estimated extravascular $T_{2E}^{*} = 50$ ms (with equal spin densities).

The BOLD signal model developed here is similar to, but not identical to, other proposed signal models (e.g., the model proposed by Davis et al., 1998). The primary advantage of the current formulation is that it is explicitly based on considering independently the intravascular and extravascular contributions. Because of this, the model can readily be applied to experiments in which the intravascular component is deliberately suppressed by applying diffusion-weighting gradients to kill the blood signal. On the other hand, the fact that extravascular and intravascular effects are lumped into one scaling parameter M in the Davis model is more convenient for calibrated BOLD experiments in which hypercapnia is used to estimate M (Davis et al., 1998). In most applications, either the Davis model or the current model could be used with similar results.

In this formulation, the BOLD signal change is a function of the normalized changes in blood volume and blood oxygenation, and a few dimensionless parameters. There are several features of this equation to note. The BOLD signal is always proportional to the fractional blood volume, so we would expect the largest signal changes to be in voxels containing veins draining an activated region. For a pure blood volume change, with no change in the oxygenation of the blood, $q = v$ and the signal change is proportional to $k_1 - k_3$. For a pure oxygenation change with constant blood volume, $v = 1$ and the signal change is proportional to $k_1 + k_2$. Finally, if the signal of blood is nulled by applying diffusion weighting gradient pulses, $\varepsilon = 0$ and this makes $k_2 = 0$ and $k_3 = -1$. For the purposes of this paper, the three k's can be replaced by two numbers a_1 and a_2, as in Eq. (2).

Note that the k's are field dependent: k_1 is proportional to the field, but k_2 and k_3 are more difficult to estimate. The intrinsic ratio of the blood to tissue signal will likely be reduced, and this will tend to reduce both k_2 and k_3. However, the slope r_0 defining the dependence of the relaxation rate on blood oxygenation is likely to be steeper, and this will tend to increase k_2. The unknown proportion of the balance of these conflicting effects makes the change in k_2 difficult to estimate. If the intrinsic blood signal is greatly reduced at high field, then only k_1 and q are important. However, this is likely not valid for 3 T and below, because diffusion-weighting experiments show that the BOLD signal can still be reduced by about one-third, indicating that the vascular signal is not zero.

References

Bandettini, P.A., Kwong, K.K., Davis, T.L., Tootell, R.B., Wong, E.C., Fox, P.T., Belliveau, J.W., Weisskoff, R.M., Rosen, B.R., 1997. Characterization of cerebral blood oxygenation and flow changes during prolonged brain activation. Hum. Brain Mapp. 5, 93–109.

Boynton, G.M., Engel, S.A., Glover, G.H., Heeger, D.J., 1996. Linear systems analysis of functional magnetic resonance imaging in human V1. J. Neurosci. 16, 4207–4221.

Buxton, R.B., 2002. Introduction to Functional Magnetic Resonance Imaging: Principles and Techniques, First ed. Cambridge Univ. Press, Cambridge.

Buxton, R.B., Frank, L.R., Wong, E.C., Siewert, B., Warach, S., Edelman, R.R., 1998a. A general kinetic model for quantitative perfusion imaging with arterial spin labeling. Magn. Reson. Med. 40, 383–396.

Buxton, R.B., Wong, E.C., Frank, L.R., 1998b. Dynamics of blood flow and oxygenation changes during brain activation: the balloon model. Magn. Reson. Med. 39, 855–864.

Cox, R.W., 1996. AFNI: software for analysis and visualization of functional magnetic resonance neuroimages. Comput. Biomed. Res. 29, 162–173.

Davis, T.L., Kwong, K.K., Weisskoff, R.M., Rosen, B.R., 1998. Calibrated functional MRI: mapping the dynamics of oxidative metabolism. Proc. Natl. Acad. Sci. U. S. A. 95, 1834–1839.

Frahm, J., Kruger, G., Merboldt, K.D., Kleinschmidt, A., 1996. Dynamic uncoupling and recoupling of perfusion and oxidative metabolism during focal brain activation in man. Magn. Reson. Med. 35, 143–148.

Glover, G.H., Lemieux, S.K., Drangova, M., Pauly, J.M., 1996. Decomposition of inflow and blood oxygen level-dependent (BOLD) effects with dual-echo spiral gradient-recalled echo (GRE) fMRI. Magn. Reson. Med. 35, 299–308.

Hoge, R.D., Atkinson, J., Gill, B., Crelier, G.R., Marrett, S., Pike, G.B., 1999. Stimulus-dependent BOLD and perfusion dynamics in human V1. Neuroimage 9, 573–585.

Janz, C., Schmitt, C., Speck, O., Hennig, J., 2000. Comparison of the hemodynamic response to different visual stimuli in single-event and block stimulation fMRI experiments. J. Magn. Reson. Imaging 12, 708–714.

Kruger, G., Kleinschmidt, A., Frahm, J., 1996. Dynamic MRI sensitized to cerebral blood oxygenation and flow during sustained activation of human visual cortex. Magn. Reson. Med. 35, 797–800.

Kruger, G., Kleinschmidt, A., Frahm, J., 1998. Stimulus dependence of oxygenation-sensitive MRI responses to sustained visual activation. NMR Biomed. 11, 75–79.

Li, D., Waight, D.J., Wang, Y., 1998. In vivo correlation between blood T2* and oxygen saturation. J. Magn. Reson. Imaging 8, 1236–1239.

Liu, T.T., Luh, W.M., Wong, E.C., Frank, L.R., Buxton, R.B., 2000. A method for dynamic measurement of blood volume with compensation for T2 changes. Eight Meeting, International Society for Magnetic Resonance in Medicine, Denver, p. 52.

Mandeville, J.B., A. Marota, J.J., Kosofsky, B.E., Keltner, J.R., Weissleder, R., Rosen, B.R., Weisskoff, R.M., 1998. Dynamic functional imaging of relative cerebral blood volume during rat forepaw stimulation. Magn. Reson. Med. 39, 615–624.

Mandeville, J.B., Marota, J.J., Ayata, C., Zaharchuk, G., Moskowitz, M.A., Rosen, B.R., Weisskoff, R.M., 1999. Evidence of a cerebrovascular postarteriole windkessel with delayed compliance. J. Cereb. Blood Flow Metab. 19 (6), 679–689.

Miller, K.L., Luh, W.M., Liu, T.T., Martinez, A., Obata, T., Wong, E.C., Frank, L.R., Buxton, R.B., 2001. Nonlinear temporal dynamics of the cerebral blood flow response. Hum. Brain Mapp. 13, 1–12.

Nakai, T., Matsuo, K., Kato, C., Takehara, Y., Isoda, H., Moriya, T., Okada, T., Sakahara, H., 2000. Post-stimulus response in hemodynamics observed by functional magnetic resonance imaging—Difference between the primary sensorimotor area and the supplementary motor area. Magn. Reson. Imaging 18, 1215–1219.

Obata, T., Liu, T.T., Miller, K.L., Luh, W.-M., Wong, E.C., Frank, R.B., Buxton, R.B., 2000. BOLD overshoots at task-switching points in supplementary motor area. Eighth Meeting, International Society for Magnetic Resonance in Medicine, Denver, p. 500.

Ogawa, S., Menon, R.S., Tank, D.W., Kim, S.-G., Merkle, H., Ellerman, J.M., Ugurbil, K., 1993. Functional brain mapping by blood oxygenation level-dependent contrast magnetic resonance imaging: a compar-

ison of signal characteristics with a biophysical model. Biophys. J. 64, 803–812.

Wong, E.C., Buxton, R.B., Frank, L.R., 1997. Implementation of quantitative perfusion imaging techniques for functional brain mapping using pulsed arterial spin labeling. NMR Biomed. 10, 237–249.

Wong, E.C., Buxton, R.B., Frank, L.R., 1998a. Quantitative imaging of perfusion using a single subtraction (QUIPSS and QUIPSS II). Magn. Reson. Med. 39, 702–708.

Wong, E.C., Buxton, R.B., Frank, L.R., 1998b. A theoretical and experimental comparison of continuous and pulsed arterial spin labeling techniques for quantitative perfusion imaging. Magn. Reson. Med. 40, 348–355.